Fire Technology manuscript No.
(will be inserted by the editor)

Design of an ASTM E119 fire environment in a large compartment*

Chao Zhang · William Grosshandler · Ana Sauca · Lisa Choe

Received: date / Accepted: date

* Cite this paper as: Zhang, C., Grosshandler, W., Sauca, A., Choe, L.. Fire Technol (2019). https://doi.org/10.1007/s10694-019-00924-7

C. Zhang
National Institute of Standards and Technology, Fire Research Division, USA
Corresponding author. E-mail: chao.zhang@nist.gov
W. Grosshandler
National Institute of Standards and Technology, Fire Research Division, USA
A. Sauca
National Institute of Standards and Technology, Fire Research Division, USA
L. Choe
National Institute of Standards and Technology, Fire Research Division, USA

Abstract Structural fire protection design in the United States is based on prescriptive fire-resistance ratings of individual load-bearing elements which are derived from standard fire testing, e.g. ASTM E119. In standard fire testing, a custom-built gas furnace is traditionally used to heat a test specimen by following the gas temperature-time curve prescribed in the ASTM E119 standard. The span length of the test specimen seldom exceeds 6 m due to the size limitations of available furnaces. Further, the test specimen does not incorporate realistic structural continuity. This paper presents a basis for designing an ASTM E119 fire environment in a large compartment of about 10 m wide, 7 m deep and 3.8 m high constructed in the National Fire Research Laboratory of the National Institute of Standards and Technology. Using the designed fire parameters, a full-scale experiment was carried out on December 20, 2018. The measured average upper layer gas temperature curve was consistent with the E119 fire curve. The maximum difference between the measured curve and the E119 fire curve towards the end of the test was about 70 °C (7%). The study indicates that by proper design and control, the time-temperature curve for the standard fire testing may be approximated in a real compartment. The experimental method suggested in this paper would allow to extend the application of the standard fire testing to large-scale structures not limited by the size of furnaces, to experimentally evaluate the thermally-induced failure mechanism of structural systems including connections and frames, and to advance fire protection design methods.

Keywords Full-scale experiment · ASTM E119 fire · Large compartment · Test fire · Design approach

1 Introduction

From 1917 to 1920, the National Board of Fire Underwriters, Underwriters Laboratory, Factory Mutual companies, and the National Bureau of Standards (NBS, now the National Institute of Standards and Technology, NIST) worked together and conducted the first standardized fire tests on columns[1]. More than 100 columns made of steel, cast iron, reinforced concrete, and timber were tested [1]. Simon H. Ingberg of NBS was in charge of this program, which resulted in the establishment of the fire resistance rating method or standard fire test method in 1918 [2]. In 1928, Ingberg published "Tests of the severity of building fires" [3] in which the concept of equivalent fire severity was originally proposed. By that concept, the severity of a realistic fire was assessed based on the area under the time-temperature curve and, therefore, could be quantified by the duration in a standard fire exposure (fire resistance rating). Although the area under a fire curve does not account for the time-dependent interaction between the thermal load and the structural response, Ingberg's development of the concept of equivalent fire severity was regarded as a major milestone in the modern discipline of fire safety engineering [4]. The concept of equivalent fire severity is the basis for the fire resistance rating method or standard fire test method used in current codes. After Ingberg, alternative approaches were developed, e.g. [5–7], intending to calculate the equivalent fire severity in a more rational way. However, none of these approaches has been

[1] Note that the first known publication of the standard fire curve is NFPA Quarterly, Vol. 9 (1916), pp. 253-260.

generally accepted, mostly because of their inability to account for the behavior of structures in realistic fires. The lack of connection between fire resistance rating and the actual behavior of structures in fire remains a challenging problem in the field of fire protection research.

The fire resistance rating method has dominated fire protection design practice and has remained almost unchanged over the past 100 years [8]. The method is regarded as easily implementable, controllable and reproducible, while both accidental fires (e.g. the Broadgate Phase 8 fire [9]) and realistic fire tests (e.g. the Cardington full-scale fire tests [10]) have demonstrated that the method cannot adequately assess the actual level of safety of a structure exposed to fire. The limitations of the standard fire test method have been generally recognized and usually include the following critiques [11]: (1) the standard fire curve is not representative of a realistic fire in a real building. A realistic fire includes both heating and cooling phases while the standard fire does not decrease with time. Also, the standard fire represents a uniform heating condition while the heating condition in a realistic fire is typically non-uniform; and (2) the tested isolated members in the furnace seldom represent the behavior of the components in an entire structure. In a real building, a component is restrained by the surrounding structures. The restraints induce stress in the heated component and might also activate alternative load-bearing modes (e.g., membrane action of a composite floor slab [12], catenary action of restrained beams [13]). Furthermore, there exist alternative load paths in entire structures [14].

Over the past few decades, especially after the Cardington full-scale fire tests [10], a large amount of effort has been devoted to research on performance-based methods for fire protection design. Most work has been conducted in furnaces using the standard fire curve or other user-defined fire curves [15–21], while compartment fire tests [8, 22] and open burning/heating tests [23, 24] have also been conducted. Furthermore, collapses of buildings in actual fires (e.g. the World Trade Center [25] and the Faculty of Architecture Building at Delft University of Technology [26]) present that structural performance in realistic fires is deemed more complex than those observed in furnace tests. For situations where the effect of fire induced thermal gradient is significant, fire protection design based on the furnace tests might not be conservative [27–30]. Therefore, testing structures in realistic fires becomes a priority in moving towards structural fire engineering design [31], and the development of novel fire testing methods has become an important research topic [32–34]. A notable achievement of realistic fire testing is the construction of a unique facility: the National Fire Research Laboratory (NFRL) at the National Institute of Standards and Technology [35]. The NFRL currently is the only facility in the United States that allows research on the response of real-scale structural systems to a realistic fire simultaneously with mechanical loading under precisely controlled laboratory conditions.

A significant need still exists for a fuller understanding of the failure mechanisms of structural systems in fire and for advancement of current design methods, both prescriptive and performance-based. Since standard fire testing was first introduced, structural testing techniques, computational modeling and fire safety science have evolved, allowing the high-fidelity modeling and testing of the performance of structural systems in realistic fires. With the unique facilities such as the NFRL and by interdisciplinary research collaborations, reliable experimental and numerical data can be produced for advancing design methods. In celebration of the 100th anniversary of the establishment of the standard fire testing methods, e.g., the China-US Workshop on Building Fire Safety (held on May 15, 2017 in Beijing) [36] and the ASTM Workshop on Advancements in Evaluating the Fire Resistance of Structures (held on December 6-7, 2018 in Washington DC) [37], the capability of producing the standard fire time-temperature curve outside of a furnace, which is presented in this paper, provides an important step forward to help relate standard furnace test results to structure performance in a real fire and to advance fire protection engineering.

2 Background

NIST hosted three stakeholder workshops [31, 38, 39] to prioritize the needs of structural-fire experimental research. Based on the workshops' recommendations, composite floor systems were selected for study because of their widespread use in building construction and because of modeling challenges in such systems exposed to a fire. Long-span steel-concrete composite beams were tested in the first phase of the program. The results of these simulations and experiments are documented in [40]. The current paper deals with designing test fires for a 10 m by 7 m steel-concrete composite floor.

The test frame for this study is a two-story, two bay by three bay gravity frame, as shown in Figure 1. The test bay is 6.1 m by 9.1 m. The test bay will be loaded mechanically using hydraulic actuators to simulate the gravity service load condition. For this series of composite floor tests, the columns will not play a role in floor failure; rather, the columns will be protected so that they provide a reliable load path.

3 Design objective and procedure

Two test fires will be used, a "realistic" fire and a "standard" fire. The "realistic" fire is intended to represent an extreme but plausible fire, one that has the potential to threaten the structure. This fire will be confined within a single compartment, allowing flame leakage through openings with restricted sizes and locations. The "standard" fire will be controlled to provide uniform average upper layer gas temperatures that follow the time-temperature curve specified in the ASTM E119 standard [41]. Other conditions of the standard furnace test (e.g. pressure, heat flux distribution) are not replicated in this "standard" fire test. The results of the "realistic" fire tests will elucidate the failure modes of the floor system in a realistically restrained structural steel frame. The results from the "standard" fire tests will allow one to relate the behavior of a full-scale composite floor system to its rating provided by ASTM E119, as well as the behavior at times extended beyond its rating.

Figure 2 shows a general procedure for designing a test fire in which the temperature of an exposed steel member reaches a target temperature. The design procedure is initiated by specifying compartment geometry and boundary properties, beam specimen dimensions, insulation thickness and properties, and target steel temperature. We endeavor to solve for the heat release rate (and the size and distribution of the burners) and opening condition (size, geometry and location). First, initial values of heat release rate (HRR) and opening factor (F_o) are assumed based on literature survey. Second, simple empirical equations (e.g. parametric fire model [42] and a one-dimensional (1D) heat conduction model [43]) are used to calculate the gas and steel temperatures. If the calculated maximum steel temperature is less than the target value, the HRR and F_o are modified, as necessary. Third, a zone model and two-dimensional (2D) heat conduction analyses are used to check and refine the HRR and F_o from the previous step. Finally, a field fire model and three-dimensional (3D) heat conduction simulation are carried out to check and refine the HRR and F_o, and to optimize the size and location of the fire and vents.

The procedure outlined in Figure 2 was used previously to design the test fire for structural experiments on a 6 m long steel W-shape beam during the commissioning of the NFRL [34]. In this study, only the average gas temperature in the compartment was considered and therefore the heat conduction analyses for the exposed members was not be performed.

4 Design of the "realistic" fire

4.1 Fire load

The heat release rate for the "realistic" fire is based upon knowledge gained in previous full-scale experiments, one conducted at NIST using three workstations as the fuel [44], and another at Cardington using wood pallets for fuel [45].

The previous full-scale fires at NIST [44] were conducted in a room that was 10.81 m deep, 7.02 m wide, and 3.36 m high. The room was fully enclosed except for windows along one of the 7.02 m walls, providing a total area of 4.77 m^2 for ventilation. Two experiments (test 1 and test 2 in [44]) were run using three identical workstations with a total combustible mass of 1670 kg (17 MJ/kg). The test at Cardington [45] was conducted in an eight-story steel structure. The fire room in Test 7 was 11.0 m wide by 7.0 m deep and one story (4.1 m) high. A single vent of 1.27 m high and 9 m wide was used. Wood cribs uniformly distributed across the floor were used as the fuel, providing 40 kg/m^2 mass load on the fire floor (700 MJ/m^2 energy load).

For the current experimental series, the fire compartment is about 10 m wide, 7 m deep and 3.8 m high, as shown in Figures 3 and 4. Four natural gas burners each 1.0 m by 1.5 m provide the fire source. Natural gas is used since: (a) a gaseous fuel allows independent and near-instantaneous control of HRR during an experiment; (b) the NFRL has extensive experience with high accuracy flow rate measurements and independent means of HRR calculation when using natural gas; (c) the major constituent of natural gas (CH_4) has the lowest tendency to soot of any hydrocarbon, providing a favorable environment for optical measurements of displacement; (d) natural gas fires are well-suited for simulation; and (e) natural gas provides a baseline for comparison to future solid fuel fires.

Surveys [46] have found that the fuel loads in commercial and public spaces vary greatly with the designated purpose of the space. A standard office contains in the range of 420 to 655 MJ/m^2 of combustible material; a shopping center is in the range of 600 to 936 MJ/m^2; and a library can have fuel loads up to

2340 MJ/m^2. The previous NIST experiment [44] with a fuel load of 400 MJ/m^2 was conducted with only three workstations in a space that more typically would have had six workstations. In such a case the energy content would have been 800 MJ/m^2, about equal to the fuel load in the Cardington tests [45] and a bit above the survey levels for typical office layouts. Because the "realistic" fire represents an extreme fire condition, an equivalent fuel load of 1.6 times the energy content more typical of a modern office, or about 1200 MJ/m^2 was proposed to simulate uncontrolled burning of building contents.

The right-hand vertical scale of Figure 5 shows the HRR for the "realistic" fire, which linearly ramps up to 10,000 kW in 15 minutes, is held steady until 105 min, and then is reduced linearly to zero over the next 85 minutes. The HRR determined by the concept given by Vassart et al. [46] is also presented for comparison purpose. The peak intensity of the fire on a volumetric basis is 37.9 kW/m^3, close to that in the previous NIST studies [44].

4.2 Opening factor

The "realistic" fire is designed to maximize the upper layer temperature, to minimize the level of smoke, and to avoid excess fuel feeding a fire external to the bay. The ventilation is controlled by the total opening area, A_o, and the height of the opening, H_o. In wood crib fueled compartment fires, when $A_o H_o^{1/2}$ is greater than 10 m$^{5/2}$, an over-ventilated condition exists [47]. Table 1 gives the key fire parameters for the previous NIST and the Cardington fire tests. W, D and H are width, depth and height of the compartment, respectively; W_o is width of the opening; V is volume of compartment; A_f and A_t are areas of floor and internal compartment boundaries (including openings), respectively; $F_o = A_o {H_o}^{1/2} {A_t}^{-1}$ is opening factor; q_f is fire load density (per unit floor area); and T_g is gas temperature. It appears that the fire in the Cardington test may have been over-ventilated, while the fire in the NIST 2008 study was under-ventilated.

Table 1 also gives the key fire parameters for the proposed "realistic" fire. When scaled with the room volume, the opening area is similar to the opening area/volume used in the over-ventilated Cardington fire. The value of $A_o H_o^{1/2}$ for the "realistic" fire suggests that this fire would be over-ventilated; however, the correlation for wood crib fires is not directly applicable to natural gas fires.

Figure 5 shows the predicted gas temperature for the proposed "realistic" fire using the parametric fire model given in the eurocode 1 (EC1) [42]. The predicted peak gas temperature is 1269 °C, significantly higher than the measured (average) gas temperature in the previous NIST [44] and Cardington tests [45] as listed in Table 1. Following the design procedure given in Figure 2, calculations using the zone model CFAST (Consolidated Model of Fire Growth and Smoke Transport) [48] were run to check the proposed HRR and opening factor. Calculations based on CFAST show that the proposed HRR and opening factor are sufficient to substantially exceed the minimum target temperature of 1000 °C, as shown in Figure 6. Figure 6 also shows that the opening configuration (location and distribution) has modest effect on the upper layer gas temperature and the layer height (i.e., the distance from the bottom of hot gas layer to the floor). The differences among the predicted peak temperatures are within 110 °C (8%) for the investigated cases. The authors are aware that zone models are incapable of considering effects of the opening configuration; however, zone model calculations still provide valuable information for the initial design of the openings for the fire compartment.

4.3 Fire confinement

Numerical simulations using the field fire model FDS (Fire Dynamics Simulator) [49] were run to study the three-dimensional fire dynamics and to identify the distribution of openings and burners for the "realistic" fire that confine the majority of the heat release to within the compartment. The heat release rate vs. time as proposed in Figure 5 is used for all of these simulations. The main opening in the south wall is 6 m wide and 1.5 m high and remains constant in size for all of the geometries examined, although height of the window sill is varied. The size and location of the opening on the opposite (north) wall, and the number and distribution of the burners are varied.

For the compartments with a proposed opening factor of 0.045 $m^{1/2}$, the FDS simulations show that the fires are over-ventilated and the heat release is confined primarily to within the compartment. Figure 7 shows how the position and size of the north vent significantly affects the simulated flame behavior. Figure 8 shows the velocity vectors on a vertical slice through the vents of the compartment with the main opening on the south wall 1 m high above the floor, a slit on the north wall 6 m wide, 0.3 m high and sill 1 m above the floor, and four burners distributed as indicated in Figure 3. The air flow is entirely inward through the opening on the north wall. Note that the steel members (steel beams supporting the compartment ceiling slab as shown in Figure 3) are omitted in the FDS models because the heat sink effect of the steel members was found to be negligible based on the calculation by a modified one zone model [50].

4.4 Uniform gas temperature distribution

Figure 9 shows the FDS predicted temperature distributions for the compartment with the proposed HRR (produced by four distributed burners as shown in Figure 3), and a main opening on the south wall (1 m high above the floor) and an opening on the opposite north wall (6 m width, 0.3 m high and 1 m above the floor). The horizontal temperature distribution in the gas layer about 30.5 cm below the ceiling is quite uniform. Figure 10 shows the FDS predicted gas temperature-time curves. The maximum gas temperature reaches 1000 °C with the standard deviation among 35 temperature detectors located 30.5 cm below the ceiling of 50 °C. Note that there is large temperature gradient in the compartment height, as shown in Figure 9.

5 Design of the "standard" fire

5.1 Critical opening factor

The temperature-time curve in the heating phase of the EC1 parametric fire model can approximate the standard temperature-time (ISO834 fire [51]) curve if the following condition is met [42]:

$$\frac{(F_o/b)^2}{(0.04/1160)^2} = 1 \tag{1}$$

where b is the thermal inertia of the enclosure, taken as 497 $\mathrm{J/m^2s^{1/2}K}$ for the investigated compartment. From Eq. 1, we get a critical opening factor, $F_{o,cr}$,

$$F_{o,cr} = (0.04/1160)b \tag{2}$$

We assumed that in order to produce the time-temperature profile used in the standard fire the opening factor of the compartment should exceed the critical opening factor calculated by Eq. 2. For the "realistic" fire, $F_{o,cr}$ is 0.017 $\mathrm{m^{1/2}}$, which is much less than the opening factor of the compartment of 0.045 $\mathrm{m^{1/2}}$. This suggests that the ISO834 (or ASTM E119) fire environment can be produced by using the same ventilation as proposed for the "realistic" fire and adjusting the heat release rate.

5.2 Heat release rate

The maximum heat release rate for a ventilation controlled fire may be calculated simply by [52]

$$HRR_{max} = 1500 A_o \sqrt{H_o} \tag{3}$$

For the proposed ventilation, HRR_{max}=18.5 MW. For the critical opening factor given above, a critical heat release rate is calculated ($A_o\sqrt{H_o}_{cr} = F_{o,cr}A_t$) and taken as 7.0 MW. Therefore, based on the assumption given above, the maximum heat release rate for the "standard" fire should be between 7.0 MW to 18.5 MW.

In the ASTM E119 standard [41], seven points on the furnace temperature curve are used to determine the character of the curve. The same approach is adopted in this study and Table 2 gives the six points used to determine the character of the predicted fire curves. By matching the predicted temperatures with the E119 temperatures at those six points, a heat release rate time-history curve was calculated by CFAST simulations, as given in Table 2. The heat release rates between different points were determined by linear interpolation.

Figure 11 shows the average gas temperatures predicted by FDS using the HRR curve determined by CFAST simulations. The gas temperatures are taken as the average recorded values of five thermocouple devices located 30.5 cm below the ceiling. Figure 12 shows the locations of the devices. Note that because symmetry is used in the FDS simulation, the average of five thermocouple devices in the half model is equal to the average of ten thermocouple devices in the whole model. In the ASTM E119 standard [41], at least nine thermocouples placed 30.5 cm from the exposed face at the beginning of the test should be used to average the furnace temperature for floor tests. The temperature in a test specimen is determined by the heat flux or the adiabatic surface temperature at the exposed solid boundary, instead of the surrounding gas temperature (measured by the thermocouples). In furnace tests, the difference between the adiabatic surface temperature (measured by plate thermometer [53] and the gas temperature (measured by shielded thermocouple) was found to be insignificant after the initial fire exposure (8 min) [54].

Although the difference between the adiabatic surface temperature and the gas temperature in a realistic fire might be significant [55], the thermocouples are used in this study, because the objective of the "standard" fire is to provide the fire environment in the ASTM E119 standard [41]. Note that if the objective is to provide the ISO 834 fire environment, adiabatic surface temperatures at the exposed solids should be considered in FDS calculations since plate thermometers are used to control the furnace temperature in the ISO 834 standard [51]. As can be seen in Figure 12, using CFAST simulated values of HRR in FDS to calculate the average gas temperatures leads to significant under prediction of the E119 temperatures after the first 5 min.

The upper curve in Figure 11 shows the average gas temperatures predicted by FDS using the HRR values in Table 2. The most appropriate HRR was determined through a trial and error process by varying the maximum value within the range of 7 MW to 18 MW. The FDS simulations show that the "standard" fire is capable of approximating the E119 time-temperature curve. The accuracy of the proposed fire parameters (opening, HRR, etc.) is examined in the experimental investigation described in the next section.

6 Experimental investigation

On December 20, 2018 a fire test was carried out at the NFRL, using the designed compartment (and ventilation) shown in Figures 3-4 and the proposed heat release rate (and burners) for the "standard" fire predicted by FDS in Figure 11. Twelve stainless steel sheathed thermocouples were placed 30.5 cm below the ceiling, as shown in Figure 3 and Figure 12. The average of the measured temperatures by those thermocouples was used to represent the average upper layer gas temperature in the compartment. The fire test lasted 80 min. Figure 13 shows the test compartment with a view of the fire.

Figure 14 shows the measured time-temperature curves by the twelve thermocouples. The average gas temperature and the standard deviation are also presented. The maximum standard deviation is within 40 °C. Figure 15a shows the comparison between the measured average gas temperature curve with the E119 fire curve and Figure 15b shows the measured and proposed heat release rate (of the burners). Note that in the test the heat release rate of the burners was ramped about 7.5 min after ignition, and, therefore, the zeros of the X-axis in Figure 15a-b were shifted by 7.5 minutes. In the first 25 min of the test, the measured average gas temperature is slightly lower than the one specified by ASTM E119, due mostly to the lower heat release rate in the test in comparison to the proposed value, as shown in Figure 15b. The measured average gas temperature exceeds the E119 fire curve towards the end of the test, where the measured value exceeds the predicted value by 70°C (7%).

Post-test simulation using the measured heat release rate was conducted to better understand the accuracy of the proposed fire parameters. The whole compartment which includes the steel beams (shown in Figure 3) was modeled in FDS with uniform grids of 0.05 m. The FDS input file and the numerical data can be found in the FDS Github repository [2]. Figure 16 shows good agreement between

[2] https://github.com/firemodels/fds/tree/master/Validation/NIST_E119_Compartment. Accessed: 2019-07-29.

the predicted and measured average upper layer gas temperatures. At temperatures above about 700 °C, FDS under-predicted the average temperatures (within 60 °C), which might be explained by the fact that the downward deformation of ceiling was not considered in the FDS numerical model. Note that the zero of the X-axis in Figure 16 is defined at 5.75 min after ignition when the measured heat release rate of the burners steps to an initial constant value (see the "HRR_burner" green line). Figure 17 compares the measured and predicted gas temperatures by thermocouples located 30.5 cm beneath the ceiling. FDS predicts lower maximum gas temperatures on the north side of the compartment (TC7 to TC12). On the south side, FDS predicts lower or higher maximum gas temperatures (TC1 to TC6), most likely because of the impact of the main opening.

7 Conclusion

The standard fire is historically perceived to be an artificial fire, not representative of any realistic fire in a real building, due to the fact that the standard fire heating environment was originally developed from furnace tests. This study indicates that by proper design and measurement control the standard fire heating environment can be approximated in a full room compartment (70 m^2 floor plan, 3.8m high). We have found the specific fire parameters (HRR and opening condition) for this compartment and have confirmed experimentally that these fire parameters develop a nearly uniform temperature-time curve closely similar to that of the ASTM E119 fire curve. This is the first time that such curve is recreated inside a large compartment instead that inside a small compartment or furnace (note that the methodology presented in this paper could also be used to develop other standard fire conditions like ISO 834). This study also indicates that the standard temperature-time curve could be reached in fuel controlled fires.

The fire load associated with the standard temperature-time curve used in this study might not adequately represent the realistic building fires in which burning behavior of combustible contents is complex and cannot be easily predicted. However, calculations conducted in this study indicate a new way to create standard fire exposure incorporating natural gas burners. The experimental methods suggested in this paper would allow to extend the application of the standard fire testing to large-scale structures not limited by the size of furnaces, to experimentally evaluate the thermally-induced failure mechanism of structural systems including connections and steel frames, and to advance fire protection fire protection design methods. The authors are aware that the experiment method investigated in this study is one of many ways to test a structure in fire and there is no general agreement on which way is the best at the time of writing.

Acknowledgements

We thank the NFRL staff including Ramesh Selvarajah, Brian Story, Laurean DeLauter, Anthony Chakalis, Philip Deardorff, Marco Fernandez and Artur Chernovsky for their significant contributions to design, construction and execution of this test program. Valuable suggestions and review comments from Dr. Anthony

Hamins, Dr. Matthew Bundy, Dr. Matthew Hoehler, Mr. Nelson Bryner, and Dr. Hai S. Lew of NIST are acknowledged.

Disclaimer

Certain commercial entities, equipment, or materials may be identified in this document in order to describe an experimental procedure or concept adequately. Such identification is not intended to imply recommendation or endorsement by the National Institute of Standards and Technology, nor is it intended to imply that the entities, materials, or equipment are necessarily the best available for the purpose.

References

1. V. Babrauskas and R.B. Williamson. The historical basis of fire resistance testing — part i. *Fire Technology*, 14:184–194, 1978.
2. V. Babrauskas and R.B. Williamson. The historical basis of fire resistance testing — part ii. *Fire Technology*, 14:304–316, 1978.
3. S. Ingberg. Tests on the severity of building fires. *NFPA Quarterly*, 22:43–61, 1928.
4. D.R. Lide. A century of excellence in measurements, standards and technology. NIST Special Publication 958, National Institute of Standards and Technology, Gaithersburg, MD 20899, 2001.
5. M. Law. A relationship between fire grading and building design and contents. Fire Research Notes 877, Fire research Station, UK, September 1971.
6. O. Pettersson, S.E. Magnusson, and J. Thor. Fire engineering design of steel structures. Publication No 50, Swedish Institute of Steel Construction, Stockholm, Sweden, 1976.
7. T.Z Harmathy and J.R. Mehaffey. The normalized heat load concept and its use. *Fire Safety Journal*, 12:75–81, 1987.
8. L. Bisby, J. Gales, and C. Maluk. A contemporary review of large-scale non-standard structural fire testing. *Fire Science Reviews*, 2:1–27, 2013.
9. Steel Construction Industry Forum. Structural fire engineering: Investigation of Broadgate Phase 8 Fire. Technical Report P113, The Steel Construction Institute, UK, 1991.
10. B.R. Kirby. The behaviour of a multi-story steel framed building subjected to fire attack, experimental data. Technical report, British Steel, 2000.
11. S. Lamont. *The behaviour of multi-storey composite steel framed structures in response to compartment fires*. PhD thesis, University of Edinburgh, 2001.
12. C.G. Bailey. Membrane action of unrestrained lightly reinforced concrete slabs at large displacements. *Engineering Structures*, 23:470–483, 2001.
13. T.C.H. Liu, M.K. Fahad, and J.M. Davies. Experimental investigation of behaviour of axially restrained steel beams in fire. *Journal of Constructional Steel Research*, 58:1211–1230, 2002.
14. A.S. Usmani, J.M. Rotter, S. Lamont, A.M. Sanad, and M. Gillie. Fundamental principles of structural behaviour under thermal effects. *Fire Safety Journal*, 36:721–744, 2001.
15. T.T. Lie and V.K.R. Kodor. Fire resistance of steel columns filled with bar-reinforced concrete . *Journal of Structural Engineering - ASCE*, 122, 1996.
16. J.M. Franssen, J.B. Schleich, L.G. Cajot, and W. Azpiazu. A simple model for the fire resistance of axially loaded members – comparison with experimental results . *Journal of Constructional Steel Research*, 37:175–204, 1996.
17. W.I. Simms, D.J. O'Connor, F. Ali, and M. Randall. An experimental investigation on the structural performance of steel columns subjected to elevated temperatures. *Journal of Applied Fire Science*, 5:269–284, 1996.
18. L.H. Han, X.L. Zhao, Y.F. Yang, and J.B. Feng. Experimental study and calculation of fire resistance of concrete-filled hollow steel columns. *Journal of Structural Engineering - ASCE*, 129, 2003.

19. M. Feng, Y.C. Wang, and J.M. Davies. Structural behaviour of cold-formed thin-walled short steel channel columns at elevated temperatures. Part 1: experiments. *Journal of Constructional Steel Research*, 41:543–570, 2003.
20. H.X. Yu, I.W. Burgess, and R.J. Plank. Experimental investigation of the behaviour of fin plate connections in fire. *Journal of Constructional Steel Research*, 65:723–736, 2009.
21. G.Q. Li and S.X. Guo. Experiment on restrained steel beams subjected to heating and cooling. *Journal of Constructional Steel Research*, 64:268–274, 2008.
22. O. Vassart, C.G. Bailey, A. Nadjai, W.I. Simms, B. Zhao, T.Gernay, and J.M. Franssen. Large-scale fire test of unprotected cellular beam acting in membrane action. *Structures and Buildings*, 165:327–334, 2012.
23. Y. Hasemi, Y. Yokobayashi, T. Wakamatsu, and A. Ptchelintsev. Modeling of heating mechanism and thermal response of structural components exposed to localized fires: A new application of diffusion flame modeling to fire safety engineering. NIST internal report 6030, National Institute of Standards and Technology (NIST), Gaithersburg, Maryland, 2010.
24. L. Choe, A. Agarwal, and A.H. Varma. Steel columns subjected to thermal gradients from fire loading: Experimental evaluation. *Journal of Structural Engineering - ASCE*, 142, 2016.
25. NIST NCSTAR 1A. Federal Building and Fire Safety Investigation of the World Trade Center Disaster: Final Report on the Collapse of World Trade Center Building 7. Technical report, National Institute of Standards and Technology, Gaithersburg, Maryland, November 2008.
26. M. Engelhardt, B. Meacham, V. Kodur, A. Kirk, H. Park, van Straalen I., Maljaars J., van Weeren K., de Feijter R., and Both K. Observations from the Fire and Collapse of the Faculty of Architecture Building, Delft University of Technology. In *Structure Congress*, pages 1138–1149, 2013.
27. J. Gales. *Unbonded post-tensioned concrete structures in fire*. PhD Thesis, The University of Edinburgh, 2013.
28. C. Zhang, J.L. Gross, T.P. McAllister, and G.Q. Li. Behavior of unrestrained and restrained bare steel columns subjected to localized fire. *Journal of Structural Engineering-ASCE*, 141, 2015.
29. C. Zhang, J.L. Gross, and T. McAllister. Lateral torsional buckling of steel w-beams to localized fires. *Journal of Constructional Steel Research*, 88:330–8, 2013.
30. A. Agarwal, L. Choe, and A.H. Varma. Fire design of steel columns: effects of thermal gradients. *Journal of Constructional Steel Research*, 93:107–18, 2014.
31. J. Gross A.P. Hamins F. Sadek A. Raghunathan J.C. Yang, M.F. Bundy. International R&D Roadmap for Fire Resistance of Structures Summary of NIST/CIB Workshop. Special Publication (NIST SP) 1188, National Institute of Standards and Technology, Gaithersburg, 2015.
32. C. Maluk. *Development and application of a novel test method for studying the fire behaviour of CFRP prestressted concrete structural elements*. PhD Thesis, The University of Edinburgh, 2014.
33. H. Mostafaei. Hybrid fire testing for assessing performance of structures in fire - methodology. *Fire Safety Journal*, 58:170–179, 2013.
34. C. Zhang, L. Choe, J. Gross, S. Ramesh, and M. Bundy. Engineering approach for designing a thermal test of real-scale steel beam exposed to localized fire. *Fire Technology*, 2017.
35. M. Bundy, A. Hamins, J. Gross, W. Grosshandler, and L. Choe. Structural fire experimental capabilities at the nist national fire research laboratory. *Fire Technology*, 52:959–966, 2016.
36. C. Zhang, W. Li, J.H. Sun, J. Gross, and M. Engelhardt. China-US Workshop on Building Fire Safety: Building on a Century of Fire Resistance Rating. unpublished.
37. ASTM Workshop on Advancements in Evaluating the Fire Resistance of Structures. `https://www.astm.org/SYMPOSIA/filtrexx40.cgi?+-P+MAINCOMM+E05+-P+EVENT_ID+3501+-P+MEETING_ID+125416+sympotherinfo.frm`. Accessed: 2019-07-19. The abstracts for the workshop proceeding will be published.
38. K.H. Almand, L.T. Phan, T.P. McAllister, M.A. Starnes, and J.L. Gross. NIST-SFPE Workshop for Development of a National R&D Roadmap for Structural Fire Safety Design and Retrofit of Structures: Proceedings. NIST Interagency/Internal Report (NISTIR) 7133, National Institute of Standards and Technology, Gaithersburg, 2004.

39. K.H. Almand. Structural Fire Resistance Experimental Research – Priority Needs of U.S. Industry. Grant/Contract Reports (NISTGCR) 12-958, National Institute of Standards and Technology, Gaithersburg, 2012.
40. L. Choe, S. Ramesh, M. Seif, M. Hoehler, W. Grosshandler, J. Gross, and M. Bundy. Fire performance of long-span composite beams with gravity connections. In *Proceedings of the 10th International Conference on Structures in Fire*, 2018.
41. ASTM E119-18c. Standard test methods for fire tests of building construction and materials. Standard, ASTM International, 2018.
42. BSI. *Eurocode 1: Actions on structures - Part 1-2: General rules - Actions on structures exposed to fire*. British Standard, 2002.
43. C. Zhang and A. Usmani. Heat transfer principles in thermal calculation of structures in fire. *Fire Safety Journal*, 78:85–95, 2015.
44. A. Hamins, A. Maranghides, K.B. McGrattan, T. Ohlemiller, and R. Anleitner. Federal Building and Fire Safety Investigation of the World Trade Center Disaster: Experiments and Modeling of Multiple Workstations Burning in a Compartment. NIST NCSTAR 1-5E, National Institute of Standards and Technology, Gaithersburg, Maryland, September 2005.
45. Results and observations from full-scale fire test at BRE Cardington, 16 Jan 2003. Client Report 215-741, British Steel, 2004.
46. O. Vassart, B. Zhao, L.G. Cajot, F. Robert, U. Meyer, and A. Frangi. Eurocodes: Background and Applications Structural Fire Design. JRC Scientific and Policy Reports EUR 36698 EN, European Union, 2014.
47. K. Kawagoe. Fire behaviour in rooms. Report 27, Building Research Institute, Japan, 1958.
48. R.D. Peacock, P.A. Reneke, and G.P. Forney. CFAST - consolidated model of fire growth and smoke transport (version 7). Volume 2: users' guide. NIST Technical Note 1889v2, National Institute of Standards and Technology, Gaithersburg, Maryland, September 2017.
49. K. McGrattan, S. Hostikka, R. McDermott, J. Floyd, C. Weinschenk, and K. Overholt. *Fire Dynamics Simulator, User's Guide*. National Institute of Standards and Technology, Gaithersburg, Maryland, USA, and VTT Technical Research Centre of Finland, Espoo, Finland, sixth edition, September 2013.
50. C. Zhang and G.Q. Li. Modified one zone model for fire resistance design of steel structures. *Advanced Steel Construction*, 9:282–97, 2013.
51. ISO 834-11:2014. Fire resistance tests–elements of building construction – part 11: specific requirements for the assessment of fire protection to structural steel elements. Standard, International Organization for Standardization, 2014.
52. D. Drysdale. *An Introduction to Fire Dynamics*. John Wiley and Sons, 2st edition, 1999.
53. U. Wickstrom. The plate thermometer - a simple instrument for reaching harmonized fire resistance tests. *Fire Technology*, 30:195–208, 1994.
54. M.A. Sultan. Fire resistance furnace temperature measurements: plate thermometers vs shielded thermocouples. *Fire Technology*, 42:253–267, 2006.
55. C. Zhang, G.Q. Li, and R.L. Wang. Using adiabatic surface temperature for thermal calculation of steel members exposed to localized fires. *International Journal of Steel Structures*, 13:547–556, 2013.

Table 1 Key fire parameters

Parameter	NIST 2008 [44]	Cardington 2003 [45]	"Realistic" fire (proposed)
$W \times D \times H$	7.02 m × 10.81 m × 3.36 m	11.0 × 7.0 m × 4.1 m	7.0 m × 10.0 m × 3.8 m
$W_o \times H_o$	2.25 m × 2.12 m	9.0 m × 1.27 m	6.0 m × 1.5 m
A_f	75.89 m^2	77.0 m^2	70.0 m^2
A_t	271.59 m^2	301.6 m^2	268.2 m^2
V	254.98 m^3	315.7 m^3	263.9 m^3
A_o	4.77 m^2	11.43 m^2	9.0 m^2
A_o/V	0.019 m^{-1}	0.036 m^{-1}	0.034 m^{-1}
$A_o {H_o}^{1/2}$	6.95 $m^{5/2}$	12.88 $m^{5/2}$	11.0 $m^{5/2}$
F_o	0.026 $m^{1/2}$	0.043 $m^{1/2}$	**0.045 $m^{1/2}$
fuel package	3 workstations + 40 L of jet fuel	wood cribs	4 natural gas burners, 1m × 1.5 m each
q_f	400 MJ/m^2	700 MJ/m^2	1200 MJ/m^2
peak HRR	10,000 kW	unknown	10,000 kW
peak HRR/vol	39.2 kW/m^3	unknown	37.9 kW/m^3
peak T_g	1050 °C	1070 °C	1000 °C
fire duration	67 min	200 min	less than 240 min

**Note that the compartment for the proposed "realistic" fire in this study has a slit (6 m wide, 0.3 m high and sill 1m above the floor) which is accounted in calculating the F_o is this table.

Table 2 Calculated HRR for the "standard" fire

Time	5 min	10 min	30 min	60 min	120 min	240 min
CFAST	6.4 MW	7.6 MW	7.2 MW	7.6 MW	8.0 MW	8.4 MW
FDS	6.0 MW	8.0 MW	9.0 MW	10.0 MW	11.4 MW	11.4 MW

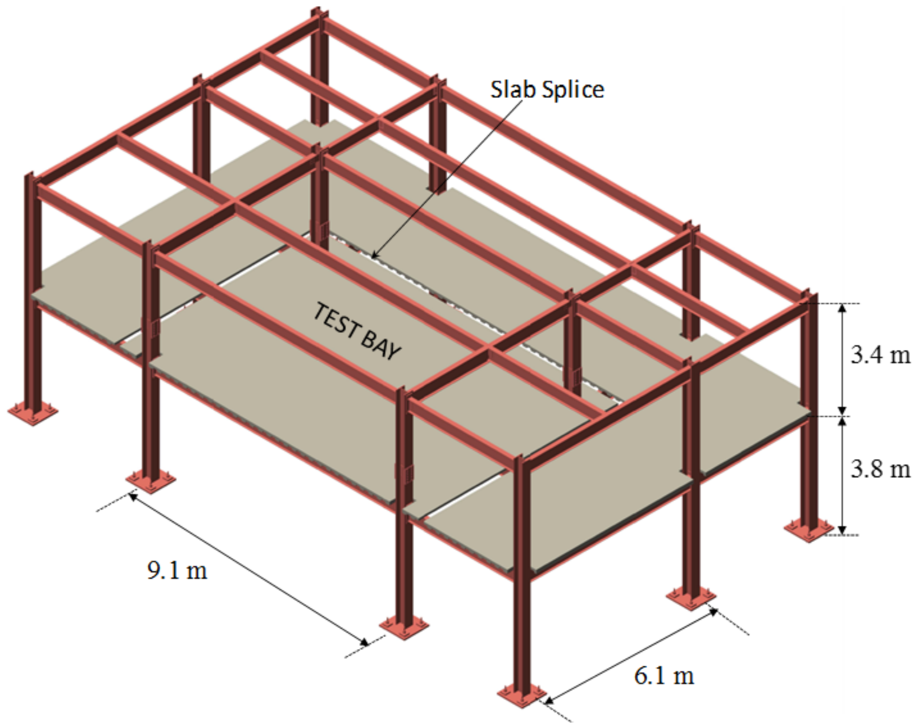

Fig. 1 Proposed test frame for the NFRL composite floor project. The compartment studied in this paper is located in the test bay.

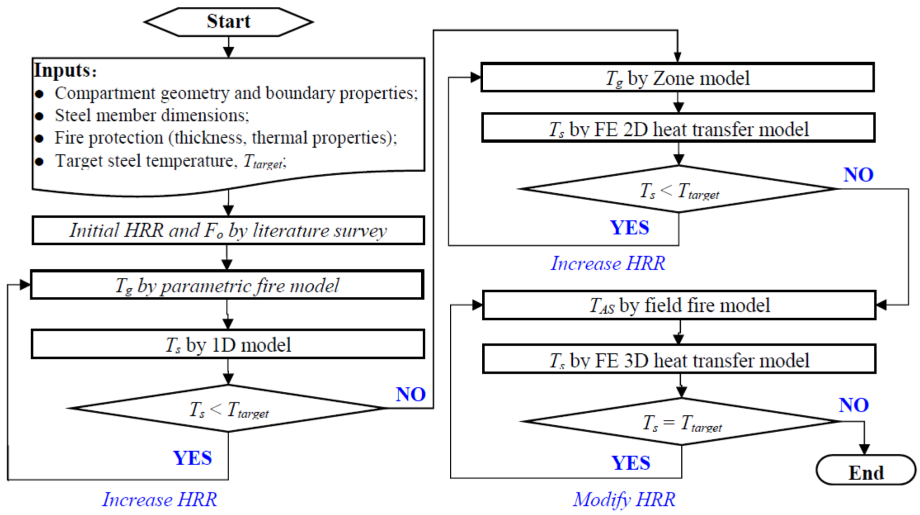

Fig. 2 Procedure for determining a heat release rate and vent configuration to reach a target temperature in a steel member exposed to fire. T_{target}, T_g, T_s and T_{AS} are target temperature, gas temperature, steel temperature and adiabatic surface temperature, respectively. HRR could vary or not vary with time, depending on the user's assumption.

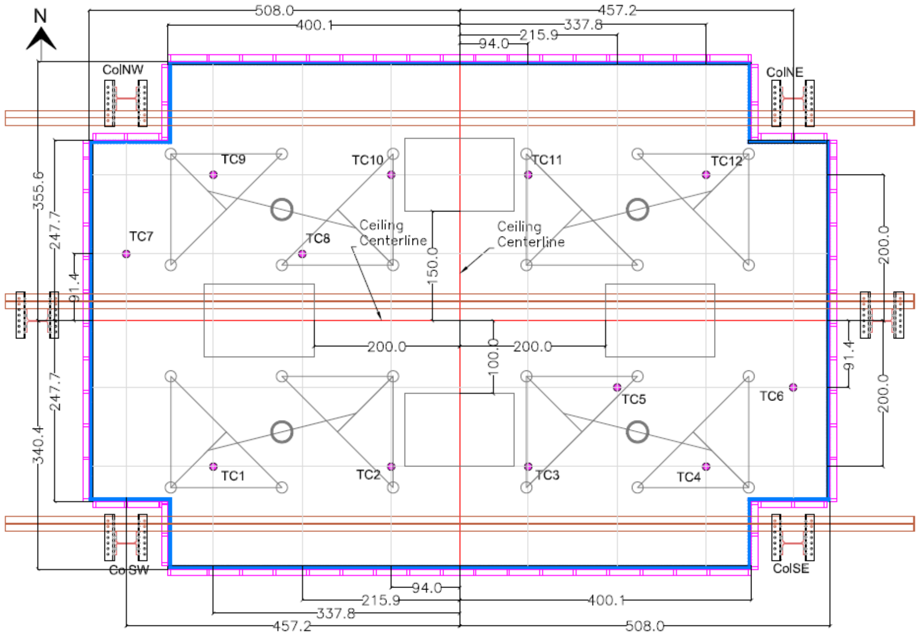

Fig. 3 Plan view of the fire compartment. TC1 to TC12 are stainless-steel sheathed thermocouples placed 30.5 cm below the ceiling (Units in cm). Four rectangular boxes are the seats for natural gas burners. Triangles show the mechanical loading systems (not included in the fire tests reported in this paper).

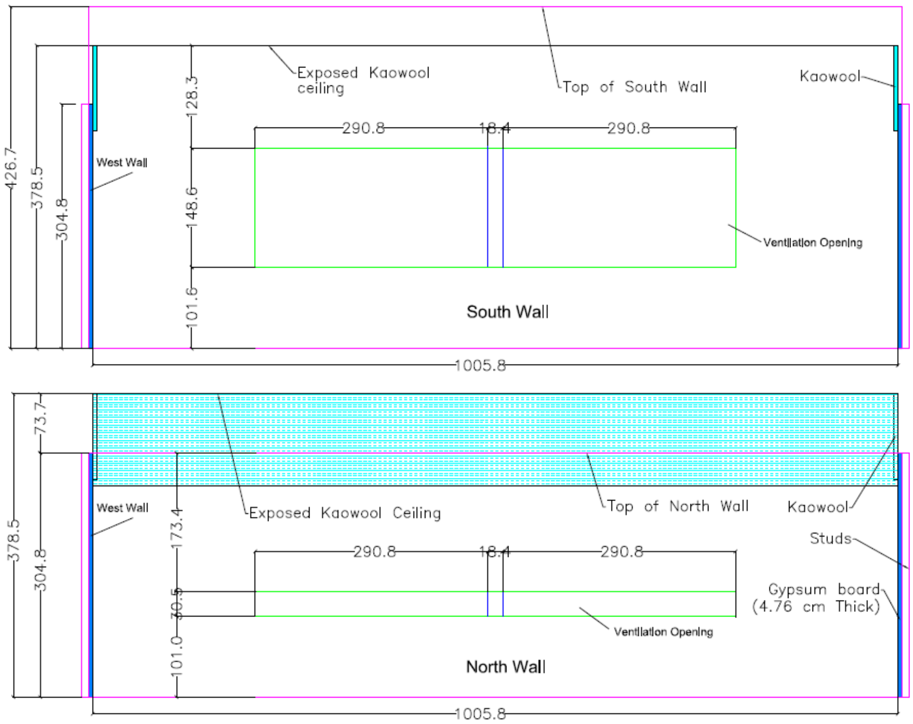

Fig. 4 Elevation view of the fire compartment (Units in cm). The compartment walls are made of stiffened sheet steel (18 gauge) protected by three layers of 16 mm thick gypsum boards and the compartment ceiling slab are made of stiffened sheet steel (20 gauge) protected by two layers of 25.4 mm thick ceramic blanket (kaowool). Two layers of 16 mm cement boards are placed on the floor of the compartment for insulation purpose.

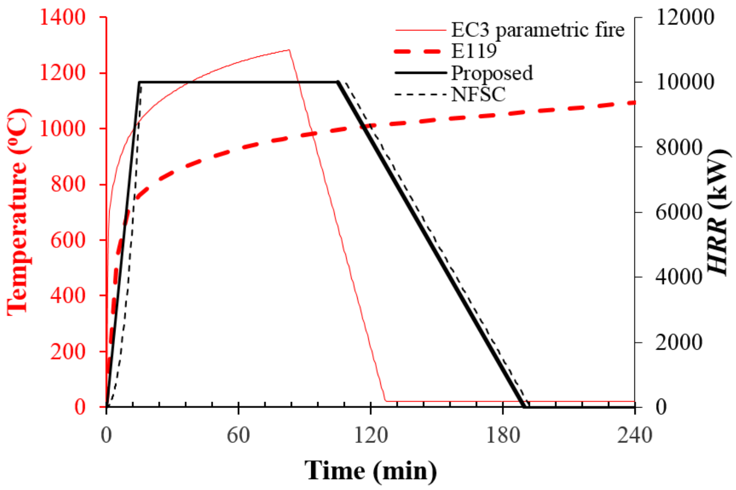

Fig. 5 Proposed HRR for the "realistic" fire and predicted gas temperature using the EC1 parametric fire model [42]. "NFSC" is the calculated HRR according to Vassart et al. [46] for medium fire growth rate. "E119" is the ASTM E119 fire curve [41]. The "Proposed" and "NSFC" HRR curves are similar and the areas below those two curves are equal. NFSC (Natural Fire Safety Concept) assumes a t-square function for the growth stage, a horizontal plateau for the steady state and a linear decreasing for the decay stage that begins when 70% of the design fire load is consumed. Note that the "NFSC" curve has a t-square ramp and the "Proposed" curve has a linear ramp.

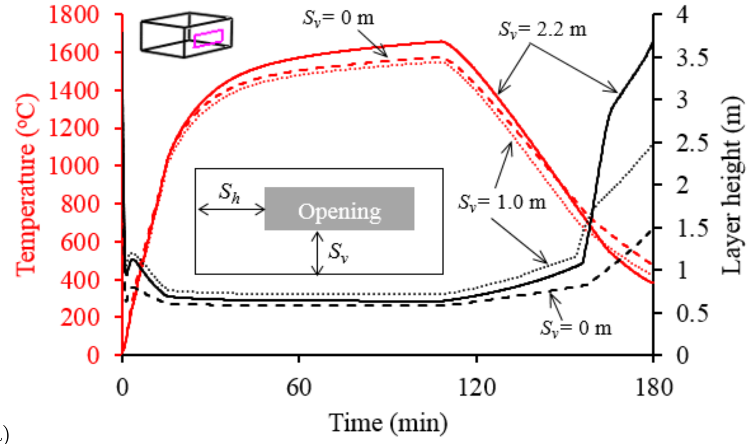

(a)

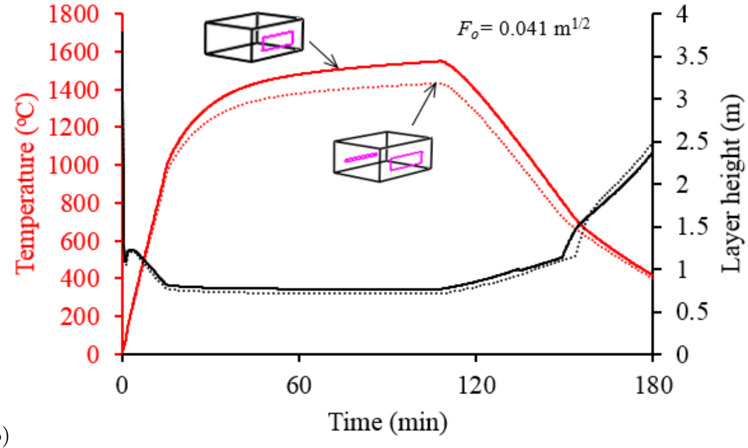

(b)

Fig. 6 CFAST predicted upper layer gas temperatures and layer heights (distance from the bottom of upper gas layer to the floor) for various opening configurations with same opening factor but at (a) different elevation and (b) different side. In (a), the opening size was held constant (6 m wide, 1.5 m high) while the elevation of the opening bottom varied (S_v) from 0 to 2.2 m. In (b), the opening factor for the case with two openings (one opening of 6 m wide, 1.383 m high in the south wall and one opening of 6 m wide, 0.3 m high in the north wall) is equal to the case with one opening (6 m wide, 1.5 m high on the south wall).

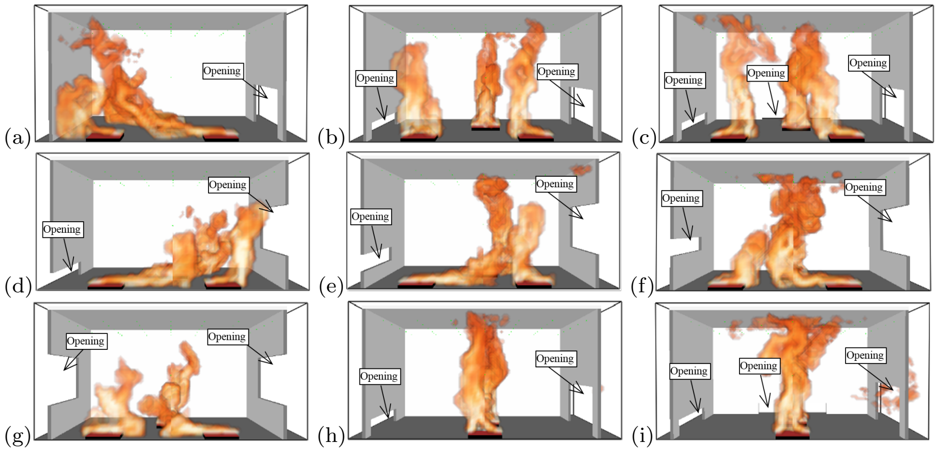

Fig. 7 Field fire model simulated flame behaviors for various opening and burners configurations. Using symmetry, only half of the compartment is modeled and the "MIRROR" boundary condition is used in the symmetry plane [49]. Uniform grids of 0.1 m are used in the XYZ directions.

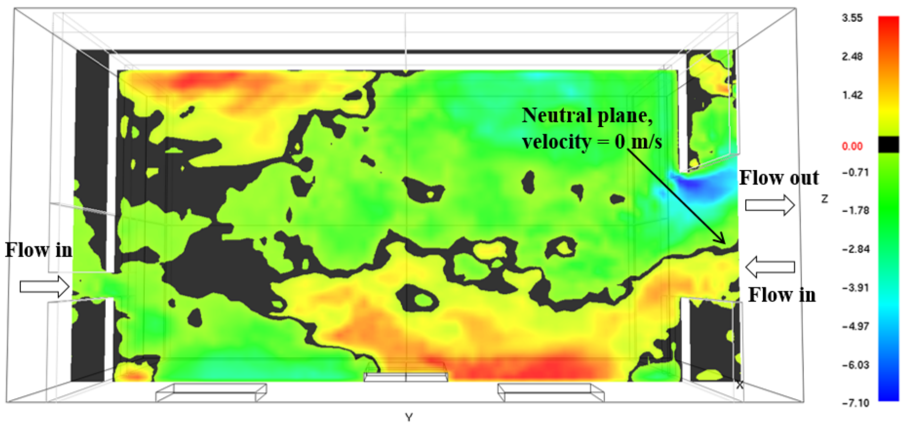

Fig. 8 Field fire model simulated velocity distribution for the compartment with a main opening on the south wall (see Figure 1) and a small opening on the opposite north wall (Units in m/s, for black areas, velocity = 0 m/s). The objects only show outlines. The vertical slice is located at 2.0 m (X=2.0 m) away from the symmetry plane.

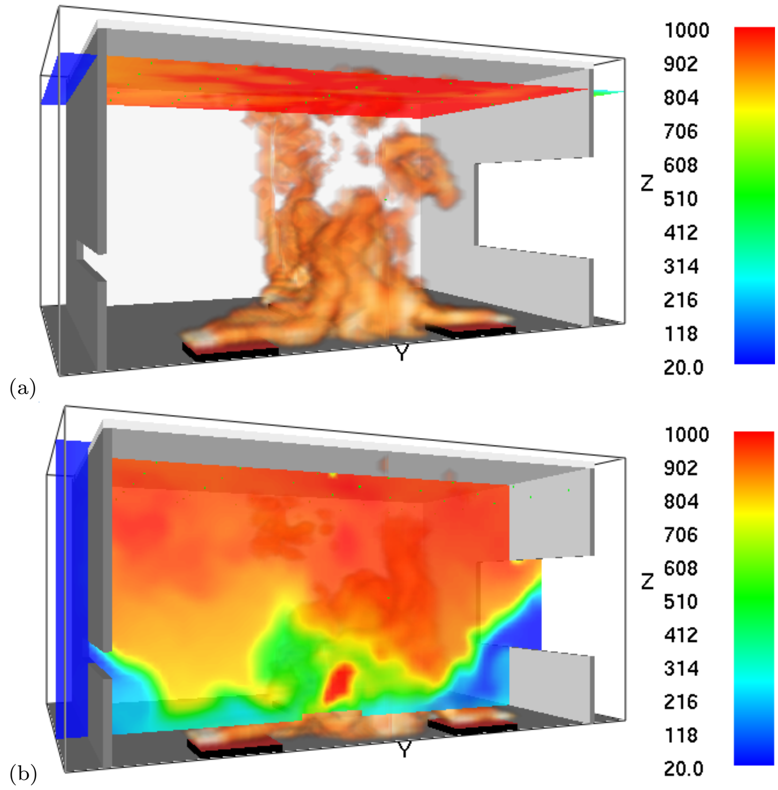

Fig. 9 Field fire model simulated temperature distributions for the compartment with proposed HRR, opening, and burners (Units in °C). The results are for fire at 1 h after burning. (a) 30.5 cm below the ceiling; (b) 2 m away from widow center.

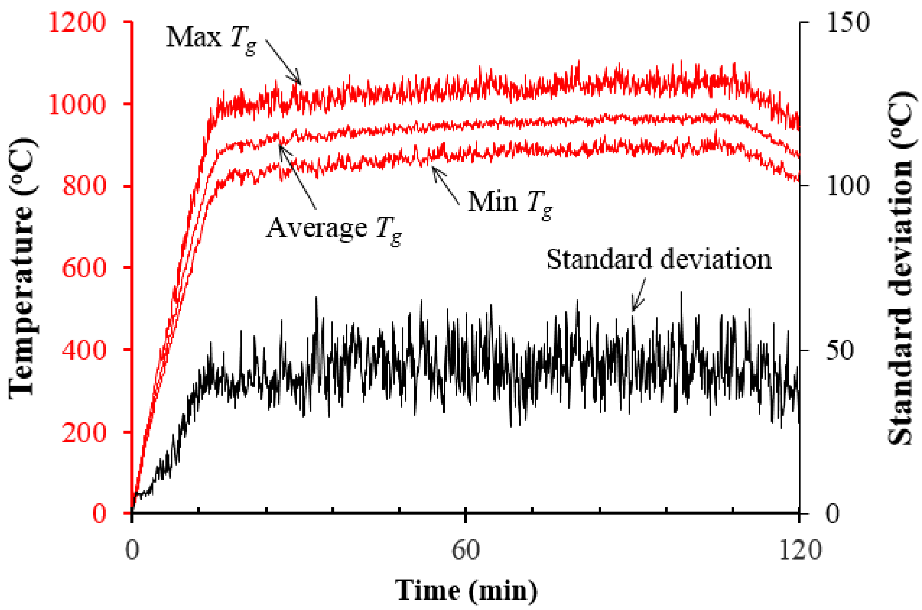

Fig. 10 Field fire model predicted gas temperatures for the compartment with proposed HRR, opening, and burners. Max, Ave and Min T_g are maximum, average, and minimum values of 35 thermocouples located 30.5 cm below the ceiling.

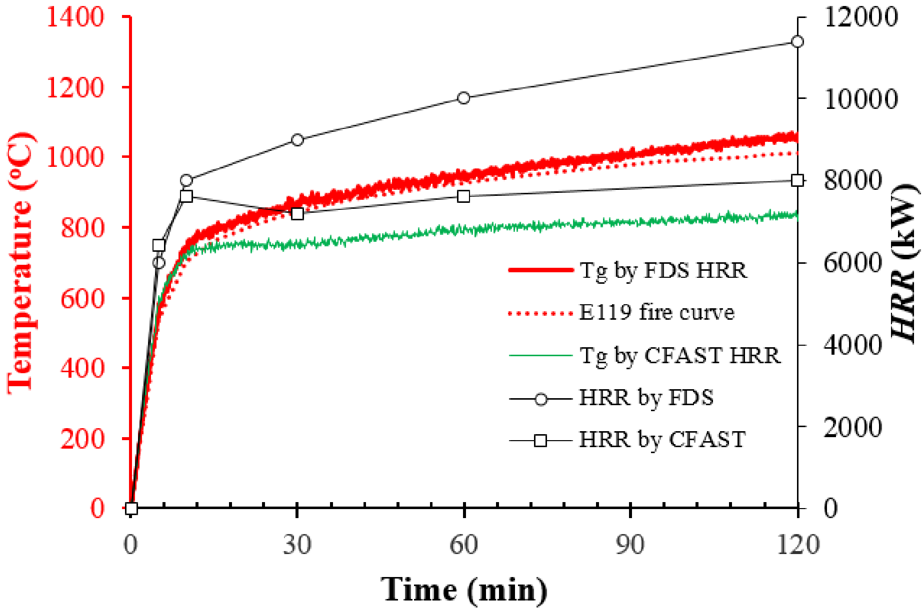

Fig. 11 FDS predicted average gas temperatures and the HRR curves calculated by CFAST and FDS. The standard deviation among 35 temperature detectors located 30.5 cm m below the ceiling is within 50 °C.

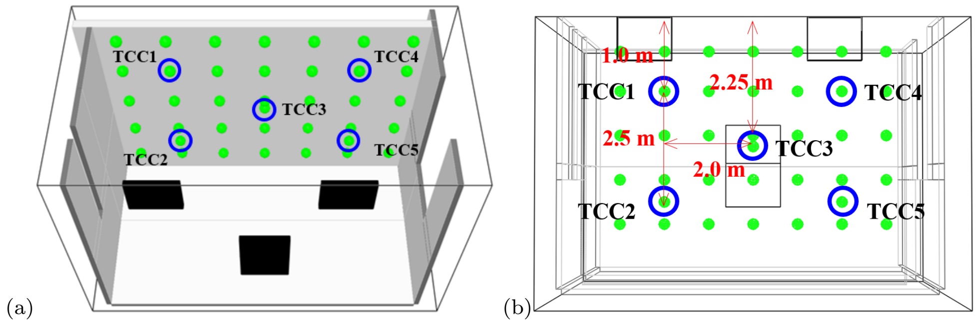

Fig. 12 Thermocouple devices used to calculate the average gas temperatures by FDS. All the devices are located 30.5 cm m below the ceiling. The circled five devices (TCC1 to TCC5) are used in the calculation. Comparison study shows that the average of these five devices is close to that of the 35 devices located 30.5 cm m below the ceiling as shown (the green points).

Fig. 13 Photographs of the test compartment. Note that the door in (c) is for construction and transportation purpose and is closed during the test.

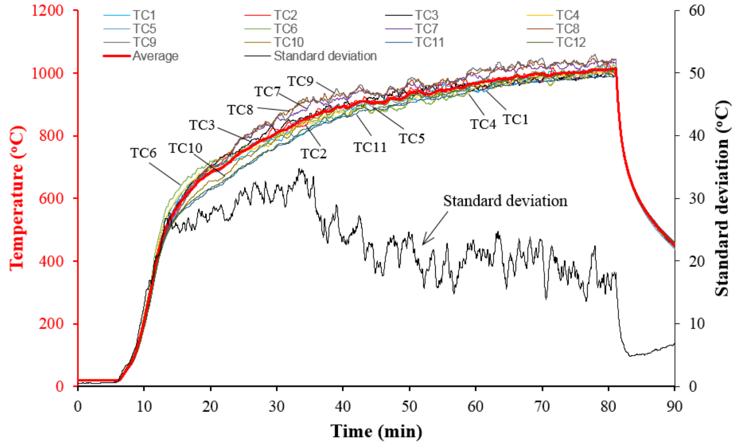

Fig. 14 Test data for twelve thermocouples.

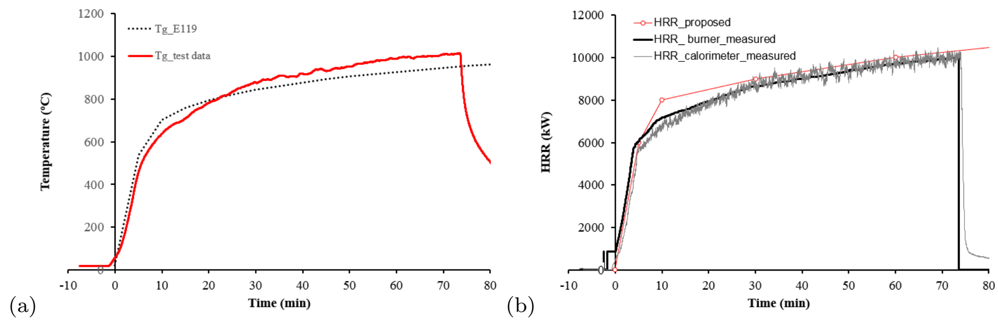

Fig. 15 (a) Comparison between measured average gas temperature curve vs the E119 fire curve; (b) Comparison between measured and proposed HRR. "calorimeter" – measured by cone calorimeter; "burner" – calculated based on natural gas flow velocity.

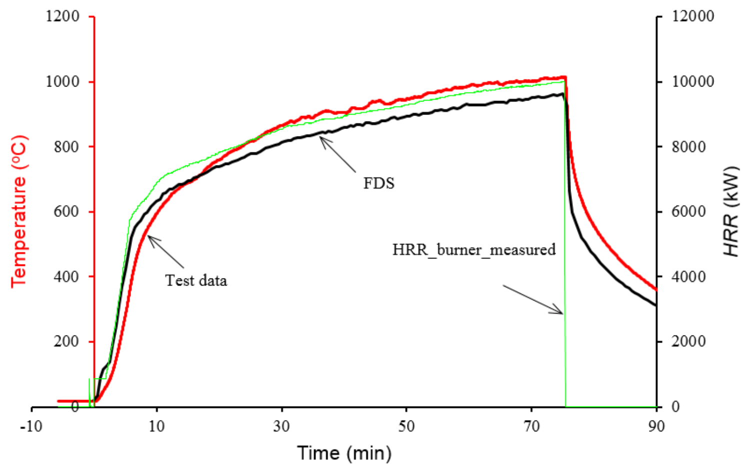

Fig. 16 Comparison between the measured average gas temperature curve vs the FDS predicted curve using the measured heat release rate (of the burner). The zero of the X-axis is shifted 5.75 min from the ignition time.

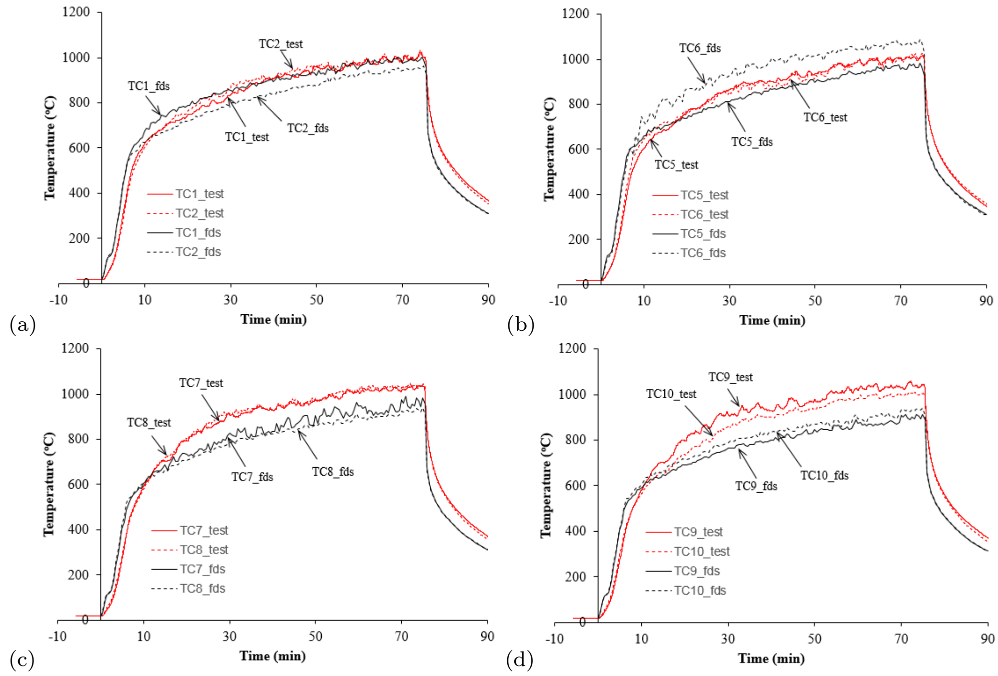

Fig. 17 Comparison between measured and predicted gas temperatures by thermocouples located 30.5 cm beneath the ceiling. The zero of the X-axis is shifted 5.75 min from the ignition time. Data for TC3, TC4, TC11 and TC12 are not show for symmetry reason.